Glycoconj J (2008) 25:199–212
DOI 10.1007/s10719-007-9071-y

Glycomic mapping of *O*- and *N*-linked glycans from major rat sublingual mucin

Shin-Yi Yu · Kay-Hooi Khoo · Zhangung Yang · Anthony Herp · Albert M. Wu

Received: 9 April 2007 / Revised: 26 August 2007 / Accepted: 29 August 2007 / Published online: 22 September 2007

Abstract Carbohydrate moieties of salivary mucins play various roles in life processes, especially as a microbial trapping agent. While structural details of the salivary *O*-glycans from several mammalian sources are well studied, very little information is currently available for the corresponding *N*-glycans. The existence of *N*-glycans alongside *O*-glycans on mucin isolated from rat sublingual gland has previously been implicated by total glycosyl compositional analysis but the respective structural data are both lacking. The advent of facile glycomic mapping and sequencing methods by mass spectrometry (MS) has enabled a structural reinvestigation into many previously unsolved issues. For the first time, high energy collision induced dissociation (CID) MALDI-MS/MS as implemented on a TOF/TOF instrument was applied to permethyl derivatives of mucin type *O*-glycans and *N*-glycans, from which the linkage specific fragmentation pattern could be established. The predominant *O*-glycans carried on the rat sublingual mucin were defined as sialylated core 3 and 4 types whereas the *N*-glycans were determined to be non-bisected hybrid types similarly carrying a sialylated type II chain. The masking effect of terminal sialylation on the tight binding of rat sublingual mucin to Galβ1→4GlcNAc specific lectins and three oligomannose specific lectins were clearly demonstrated in this study.

Keywords Lectin binding · *N*-glycans · Rat sublingual gland · Salivary mucin · Mass spectrometry

Abbreviations

ASG	armadillo salivary gland
BSM	bovine submandibular glycoprotein
ELLSA	enzyme-linked lectinosorbent assay
OSM	ovine submandibular glycoprotein
PSM	porcine salivary glycoprotein
RSL	rat sublingual glycoprotein
Tn	GalNAcα1→Ser/Thr
type I	Galβ1→3GlcNAc, or lacto-*N*-biose I
type II	Galβ1→4GlcNAc, or *N*-acetyllactosamine

Introduction

Saliva has been attributed multiple protective functions, especially in modulating microbial flora. Most of its biological properties are dependent on the glycan structures of its constituent mucins, which are collectively secreted by different salivary glands including the major parotid, submandibular and sublingual glands. Current glycomic approaches aim primarily to define the glycan expression profile of a particular biological source in order to provide a glyco-phenotypic basis to delineate the regulated expression of the implicated glycosyltransferases in relation to developmental and/or signaling programs. While biological

S.-Y. Yu · K.-H. Khoo
Institute of Biochemical Sciences, National Taiwan University, Taipei 106, Taiwan

K.-H. Khoo (✉)
National Core Facilities for Proteomics and Institute of Biological Chemistry, Academia Sinica,
Nankang,
Taipei 115, Taiwan
e-mail: kkhoo@gate.sinica.edu.tw

Z. Yang · A. Herp · A. M. Wu (✉)
Glyco-Immunochemistry Research Laboratory,
Institute of Molecular and Cellular Biology,
Chang-Gung University,
333, Kwei-san Tao-yuan, Taiwan
e-mail: amwu@mail.cgu.edu.tw

fluids are valid targets for such investigation, especially in attempts to derive non-invasive diagnostic and prognostic markers, a fundamental problem resides in their content being derived from mixed sources. In the case of salivary mucins, detailed dissection of their regulated biosynthesis entails a confident identification of the contributing glands and their respective glycosylation potentials.

For practical reasons, structural characterization of human salivary mucins is mostly restricted to total or the submandibular–sublingual saliva collected from donors as sample sources [1–6]. In contrast, investigation of mucous glycoproteins from a defined salivary gland of animal origins has been initiated as early as the 1970s [7, 8]. These investigations along with a body of other works contributed much to our current understanding of the various core type structures for mucin-type *O*-glycosylation [9, 10]. Typically, the *O*-glycans constitute over 40% of the molecular mass of mucins and occur clustered together in "mucin domains" [11, 12]. In early reports, absence of *N*-linked glycans was considered as a distinct salivary mucin feature [7]. Since then, however, several salivary mucins were reported to carry *N*-glycosylation, but mostly based on variable amounts of mannose content detected and not defined structures [1, 13, 14]. It remains unclear to summarize if the salivary mucins secreted by a particular gland carry a distinctive *N*-glycosylation pattern.

To date, only a single report has provided indirect evidence for the structures of *N*-glycans on mouse mucin isolated directly from its submandibular gland. Intriguingly, it was shown that approximately 50% of the *N*-glycans are high mannose type, dominated by a single $Man_5GlcNAc_2$ structure, while the rest comprises mainly non-bisected hybrid type, carrying 1–2 fully sialylated antenna on the 3-arm [15]. In rat, the sialylated mucins have been shown to be derived mainly from sublingual and not the submaxillary gland [7, 16]. Early work has additionally demonstrated that the major rat sublingual mucin (RSL) contained up to 2.8% of mannose by weight, indicating that the mucin synthesized and secreted by this gland contains *N*-glycans but neither the major *O*- nor the *N*-glycans have been structurally characterized [7].

Recent developments have collectively brought forth the conceptual framework of a mass spectrometry (MS)-based glycomic approach in which organized studies have shown that concerted MALDI-MS and MS/MS mapping of permethyl derivatives is one of the most efficient ways to achieve a 'first screen' profiling of high information content [17, 18]. Complementary fragmentation patterns afforded by low and high energy collision induced dissociation (CID) MS/MS have been established for the commonly occurring *N*-glycans and small bioactive oligosaccharides [19–22], which enable a highly confident sequencing of the detected glycans, complete with linkage and branching information. However, such studies have not been systematically extended to *O*-glycans. Furthermore, structural investigation of mucin glycan structures remains targeted to one glycan class or the other from a mixed biosynthetic source.

We attempt here to develop a readily implemented glycomic approach to mucin carefully isolated from a particular gland. In essence, using the RSL as a case study, we first established the characteristic features of high energy CID MALDI-MS/MS of permethylated *O*-glycans and then globally defined the overall *O*- and *N*-glycosylation profiles of rat sublingual mucin. We showed that unlike most other mucins, the RSL comprises solely *O*-glycans of core types 3 and 4 and *N*-glycans dominated by a single non-bisected, hybrid type structure, with and without core fucosylation. In both classes, a single fully sialylated type II chain dominates as the terminal sequence and epitope presented, such that binding to a panel of lectins was mostly cryptic unless first desialylated.

Materials and methods

Isolation and characterization of rat sublingual glycoprotein

Rat salivary glands, removed from the adult Sprague–Dawleys, were obtained from Pel Freeze Biologicals, Inc., Rogers, AR, as a mixture of sublingual and submandibular glands, and they were kept at −10°C until ready for use. The rat sublingual mucin was isolated according to a modified method used for the preparation of bovine and ovine submandibular mucin [16, 23]. The dissected glands, free of fat and connective tissue, were homogenized in 20 volumes of cold aqueous 0.01 M sodium chloride for 2 min and centrifuged at 12,000×*g* for 30 min. The combined clear supernatants were acidified to pH 4.8 and the denatured proteins were removed by centrifugation. The glycoproteins that remained in the supernatant were precipitated to a mucin clot by addition of 10% cetyltrimethyl ammonium bromide. The sialic acid-containing mucin clot was dissolved in 50% calcium chloride and glycoproteins were precipitated by addition of 75% ethanol. The resulting precipitate was dialyzed against distilled water, lyophilized, and then dissolved in 0.01 M, phosphate buffer, pH 6.8. Finally, the solution was subjected to batchwise treatment with hydroxylapatite. The major rat sublingual glycoprotein fraction, recovered from the supernatant fluid with homogeneous molecular weight as shown by the analytical ultracentrifugation, was designated as RSL used for this study. Desialylation of native RSL was performed by mild acid hydrolysis in 0.01 N HCl at 80°C for 90 min [23] and dialyzed for 2 days against frequently changed water. The nondialyzable material was lyophilized, designated and analyzed as asialo-RSL.

Lectins Morniga M was purified from *Morus nigra* bark by a combination of affinity chromatography and ion exchange chromatography as previously described [24]. *Ricinus communis* agglutinin 1 (RCA_1, RCA_{120}), *Pisum sativum* agglutinin (pea, PSA), *Lens culinaris* lectin (Lentil, LCL) were purchased from Sigma Chemical Company (St. Louis, MO, USA). *Erythrina cristagalli* lectin (coral tree, ECL), *Erythrina corallodendron* lectin (ECorL) were purchased from Vector Laboratories (Burlingame, CA, USA). Biotinylation of lectins was performed as described previously [25].

Glycoproteins and glycan standards Fetuin (Sigma) which is the major glycoprotein in fetal calf serum, has six oligosaccharide side chains per molecule, three *O*-linked to Ser/Thr and three *N*-linked to Asn [26]. The two major *O*-glycans were characterized as NeuAcα2-3Galβ1-3GalNAc and NeuAcα2-3Galβ1-3(NeuAcα2-6)GalNAc [27].

Human Ovarian Cyst sample #350 (HOC350) was obtained as described previously [28], from which a disialylated Core 2 *O*-glycan, NeuAcα2-3Galβ1-3(NeuAcα2-3Galβ1-4GlcNAcβ1-6)GalNAc was released and identified.

The microtiter plate lectin-enzyme binding assay Enzyme-linked lectinosorbent binding assay (ELLSA) was performed according to the procedures described [25, 29]. The volume of each reagent applied to the plate was 50 μl/well, and all incubations, except for coating, were performed at room temperature (20°C). The reagents, if not indicated otherwise, were diluted with TBS containing 0.05% Tween 20 (TBS-T). TBS buffer or 0.15 M NaCl containing 0.05% Tween 20 was used for washing the plate between incubations.

The 96-well microtiter plates (Nunc, MaxiSorp, Vienna, Austria) were coated with glycoproteins in 0.05 M carbonate buffer, pH 9.6, and incubated overnight at 4°C. After washing the plate, biotinylated lectins (5 ng) were added to each well and incubated for 30 min. The plates were washed to remove unabsorbed lectin and the ExtrAvidin/alkaline phosphatase solution (Sigma, diluted 1:10,000) was added. After 1 h, the plates were washed at least four times and incubated with *p*-nitrophenyl phosphate (Sigma 104 phosphatase substrate 5 mg tablets) in 0.05 M carbonate buffer, pH 9.6, containing 1 mM $MgCl_2$ (1 tablet/5 ml). The absorbance was read at 405 nm in a microtiter plate reader, after 4 h incubation with the substrate.

All experiments were done in duplicates or triplicates, and data are presented as the mean value of the results. The standard deviation did not exceed 12% and in most experiments was less than 5% of the mean value. For the binding experiments, the control wells, where coating or addition of biotinylated lectin was omitted, gave low absorbance values (below 0.1). It showed that blocking the wells before lectin addition was not necessary when Tween 20 was present in the TBS.

Release of O- and N-glycans *O*-Glycans were released directly from RSL and standard glycoproteins in 400 μl of 1.0 M $NaBH_4$/0.05 N NaOH, for 3 days at 37°C. Reaction was terminated by adding Dowex 50X8 (H^+ form) to the solution until it stopped bubbling. After drying down, borates were removed by repeated co-evaporation with 10% acetic acid in methanol under a stream of nitrogen. Subsequently, the sample was redissolved and passed through a Dowex 50X2 (H^+ form) column in water, followed by a Bio-Gel P2 column for further desalting.

To release *N*-glycans, RSL was first reduced (dithiothreitol at 37°C for 1 h) and alkylated (iodoacetic acid at room temperature for 1 h in the dark) in 50 mM ammonium bicarbonate (pH 8.4), followed by sequential trypsin and chymotrypsin digestions at 37°C for 4 h each. After brief boiling and cooled down, the glycopeptide and peptide mixtures were incubated with PNGase F (Roche) overnight at 37°C and then passed through a C18 Sep-Pak cartridge (Waters) in 5% acetic acid, as described [30].

Desialylation and enzyme digestion Desialylation of RSL and other sialoglycoproteins was performed by mild acid hydrolysis in 0.01 N HCl at 80°C for 90 min followed by dialysis against distilled H_2O for 2 days to remove small fragments [23, 31]. For more specific release of terminal NeuAc, the RSL *O*- and *N*-glycans were digested with 50 mU of α2,3 neuraminidase from *Macrobdella decora* (Calbiochem) in 20 μl of 50 mM sodium acetate buffer, pH 6.0, at 37°C overnight. Further removal of β-Gal from desialylated RSL *O*-glycans was performed with β4-specific galactosidase from *Streptococcus pneumoniae* (Calbiochem) in 20 μl of 50 mM sodium acetate buffer, pH 6.0, at 37°C for 12 h.

MALDI-MS and MS/MS analysis All glycans were permethylated using a modified NaOH/DMSO method [30] originally described by Ciucanu and Kerek [32], prior to MS analysis. For MALDI-TOF MS glycan profiling, the permethyl derivatives in acetonitrile were mixed 1:1 with 2,5-dihydroxybenzoic acid (DHB) matrix (10 mg/ml in acetonitrile), spotted on the target plate, air-dried, and recrystallized on-plate with acetonitrile. Data acquisition was performed manually on a benchtop M@LDI LR system (Micromass) operated in the reflectron mode. MALDI-MS/MS sequencing of the permethylated glycans were performed on both Q-TOF Ultima MALDI (Water Micromass) and 4700 Proteomics Analyzer (Applied Biosystems) exactly as described before [22].

GC-MS Analysis Partially methylated alditol acetates were prepared from permethyl derivatives by hydrolysis (2 M trifluoroacetic acid, 120°C, 2 h), reduction (10 mg/ml $NaBD_4$, room temperature, 2 h), and acetylation (acetic anhydride, 100°C, 1 h). GC-MS linkage analysis was performed on a Hewlett-Packard Gas Chromatograph 6890 connected to a HP 5973 Mass Selective Detector. HP-5MS fused silica capillary column (30 m×0.25 mm, Hewlett-Packard). Samples were dissolved in hexanes and injected directly onto the column at 60°C. The column was held at 60°C for 1 min, increased to 90°C for 1 min, and then to 290°C for 25 min at a rate of 8°C/min.

Results

Native and asialo-rat sublingual glycoprotein

The rat salivary glands used for RSL preparation were of the same batch as previously reported [16]. As noted before, the chemical composition of purified major RSL differs appreciably from that of other salivary mucus glycoproteins. The carbohydrate portion, which corresponds to about 85% by weight, consists mainly of sialic acid, GlcNAc, Gal, and GalNAc in the molar ratio of 1.4:1.4:1.5:1.0. It also contains 2.8% of Man and a small amount of Fuc. About 78% of sialic acid and most of the Fuc could be removed by mild acid treatment to give an asialo-RSL sample with about 7.2% sialic acid content.

MALDI-MS mapping and sequencing of RSL *O*-glycans

MALDI-MS mapping of the permethylated glycans directly released from RSL by conventional reductive elimination revealed a relatively simple *O*-glycosylation profile, in so far as the extent of heterogeneity in size and structures is concerned (Fig. 1). A single major molecular ion signal at *m/z* 1,950 can be assigned as $[M+Na]^+$ of the composition $NeuAc_2Hex_2HexNAc_2HexNAcitol$, while that at *m/z* 1,140 corresponds to $[M+Na]^+$ of $NeuAc_1Hex_1HexNAc_1HexNA$-citol. When subjected to MALDI CID MS/MS on a Q/TOF, the preferred glycosidic cleavages gave rise to prominent B and Y ions which clearly identify a NeuAc-Hex-HexNAc-sequence on both species (data not shown but see illustrative drawings on Fig. 1). This is consistent with the detection of a single highly abundant in source cleavage oxonium type fragment ion at *m/z* 825 ($NueNAc_1Hex_1HexNAc_1^+$) in the MALDI-MS spectrum, which indicates that, apart from a NeuAc-sialylated Hex-HexNAc antennary sequence, other structural variations such as NeuGc, disialylated and/or fucosylated terminal epitopes, are not present. Thus, the

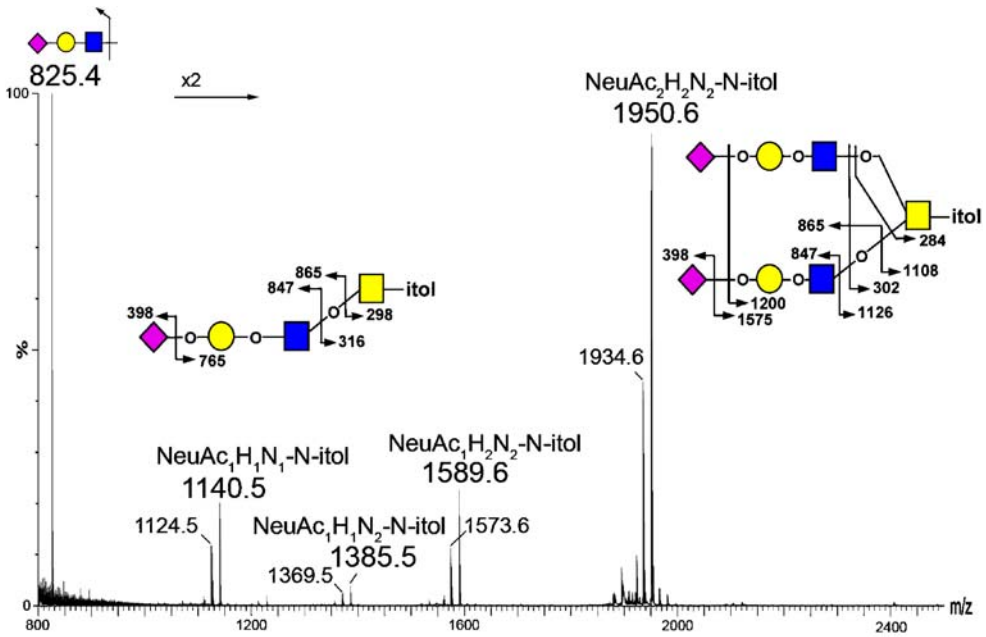

Fig. 1 MALDI-MS profile of permethylated RSL *O*-glycans. The molecular compositions of the major $[M+Na]^+$ molecular ion signals detected are assigned as labeled, and confirmed by subsequent MS/MS analyses. The assignments of the characteristic fragment ions afforded by MALDI MS/MS analysis on a Q/TOF, which allow facile determination of the sequence and branching pattern of the implicated Cores 3 and 4 *O*-glycans are schematically illustrated. Signals at 16 mass units lower than those assigned correspond to the non-reduced counterparts, the origin of which is discussed in the text. *Symbols* used here and all other MS figures: *square* HexNAc; *circle* Hex; *diamond* NeuAc. Glycosidic oxygen atoms are drawn out to discriminate between cleavages at either side of the oxygen. For peak annotation, *H* and *N* represent Hex and HexNAc respectively

smaller structure would correspond to a Core 3 *O*-glycan with a NeuAc-Gal-GlcNAc attached to GalNAcitol, whereas the major and larger structure corresponds to a Core 4 *O*-glycan with both arms substituted by the same NeuAc-Gal-GlcNAc sequence. The branch structure implicated in a Core 4 type is supported by the double cleavage $Z_{1\alpha}/Y_{1\beta}$ and $Y_{1\alpha}/Y_{1\beta}$ ions at *m/z* 284 and 302, respectively, instead of the Z_1 and Y_1 ions at *m/z* 298 and 316, as given by a Core 3 linear structure.

While a low energy CID MS/MS of permethylated glycans as implemented on a Q/TOF is sufficient to define the overall branching pattern and sequence, linkage assignment is often not possible from the glycosidic cleavage B, C, Y and Z ions, named according to the Domon and Costello nomenclature [33]. The cross ring cleavage A and X ions are useful but usually of low abundance. We and others have previously shown that a high energy CID MALDI MS/MS, as afforded by TOF/TOF, would enable linkage specific sequencing of *N*-glycans and other standard oligosaccharides if a plethora of additional cleavage ions produced can be systematically assigned [22]. Its applicability has, however, not been extended to *O*-glycans of different core types. The simple RSL *O*-glycans therefore provided valuable source samples to be examined by high energy CID MS/MS alongside other simple Core 1 and 2 *O*-glycan standards.

Fragmentation characteristics afforded by high energy CID MALDI MS/MS of *O*-glycans

The high energy CID MS/MS spectra of permethylated mono- and disialylayed Core 1 and disialylated Core 2 *O*-glycan standards are shown in Fig. 2, along with schematic illustrations of the fragment ion assignment. As noted previously, the $^{1,5}X$ ion series is reliably produced at each glycosyl residue whereas, similar to low energy CID MS/MS, the B and Y ions are found to be restricted mostly to cleavages at a HexNAc site and the terminal NeuAc. In the case of Core 1 and 2 *O*-glycans, a Z_1 ion was observed at *m/z* 298, 659 and 1,108, which define the 6-arm substituents as free, NeuAc-, and $NeuAc_1Hex_1HexNAc_1$-, respectively (Fig. 2a–c). However, the double cleavage $Z_{1\alpha}/Y_{1\beta}$ ion (*m/z* 284) was found to be much less readily afforded by *O*-glycan structures with 3,6-disubstituted GalNAcitol, as compared to under the conditions of low energy CID MS/MS on a Q/TOF.

Importantly for linkage assignment, the satellite G ions resulting from concerted elimination of C3 and C4 substituents are produced at *m/z* 472, 833 and 1,282, respectively, for cleavages at Gal, consistent with the α2–3 linkage of the attached NeuAc for each of the three standard *O*-glycans. Additional G ion equivalent can be observed at *m/z* 268, 629 and 1,078, respectively, for the concerted elimination of the NeuAc-Gal- substituent on C3 and *O*-methyl on C4 of the GalNAcitol. These and the characteristic Z_1 ions described above are sufficient to define the respective substituents on a Core 2 *O*-glycan, which would additionally give a prominent $^{3,5}A$ ion equivalent at *m/z* 935 for the entire 6-arm antennary extension (Fig. 2c). The Gal1-4GlcNAc linkage on the 6-arm can be established from the G and H ion pair at *m/z* 1078 and 1064, together with the $^{3,5}A$ ion at *m/z* 690, and D ion at *m/z* 833, which could not have derived from a type 1 Gal1-3GlcNAc linkage.

Thus, the fragmentation pattern afforded by the sialylated Core 1 and 2 *O*-glycans generally follow the rules established previously [22] although several ions appear to be more readily formed probably due to the *O*-glycans examined here being much smaller in size relative to the *N*-glycans. Notably, the highly abundant ion at *m/z* 356, which corresponds to a sodiated C_1 ion (at *m/z* 416) having eliminated the COOMe moiety, and the $^{3,5}A_1$ ion at *m/z* 254, are characteristic TOF/TOF features associated with terminal NeuAc sialylation, whereas the C_2, C_2'' and E_2 ions at *m/z* 620, 618 and 572, respectively, are typically afforded by terminal NeuAc-Gal, all of which have also been observed by others [19, 34].

Structural determination of RSL *O*-glycans

The high energy CID MS/MS profiles of the RSL *O*-glycans (Fig. 3) are similar to those of the monosialylated Core 1 (Fig. 2a) and disialylated Core 2 (Fig. 2c) *O*-glycan standards. Most importantly, the additional GlcNAc on C3 of the GalNAcitol which distinguishes Cores 3 and 4 from Cores 1 and 2 induced an extra Y_1 ion at *m/z* 316 and 1,126 for the Core 3 and Core 4 structures, respectively, apart from causing a general *m/z* shift to a HexNAc residue higher for the molecular ion and the relevant fragment ions. Thus, a Core 3 *O*-glycan is defined by the presence of a trio of G_1, Z_1 and Y_1 ions at *m/z* 268, 298 and 316, respectively. The equivalent ions are also given by Core 4 but the exact *m/z* values would be defined by the exact substituent on the 6-arm. Both Z_1 and Y_1 are also given by low energy CID MS/MS, but the G_1 ion is a unique feature of high energy CID MS/MS on a TOF/TOF. In addition, an H_1 ion equivalent (*m/z* 1,064) was also readily formed with the Cores 3 and 4 structures.

For both the major Core 3 (*m/z* 1,140) and Core 4 (*m/z* 1,950) structures of RSL *O*-glycans, the antennary sequence can be unambiguously assigned as NeuAc2-3Gal1-4GlcNAc, based on the same sets of cleavage ions described for the corresponding Cores 1 and 2 *O*-glycan standards (Fig. 2a and c). Thus, 4-linked GlcNAc is defined by the G and H ion pairs (*m/z* 513 and 499 for Core 3; *m/z* 1,323 and 1,309 for Core 4); $^{3,5}A$ ion at *m/z* 690; and D ion

at *m/z* 833, whereas the 3-linked Gal is defined by the G ion at *m/z* 717 and 1,527 for the Cores 3 and 4 structures, respectively. In support of this assignment, additional linkage analysis by GC-MS yielded 3-linked Gal, 4-linked GlcNAc and 3,6-linked GalNAcitol as the major products, with a smaller amount of 3-linked GalNAcitol (Table 1). This was further confirmed by complete removal of the NeuAc residues when the RSL *O*-glycans were treated with a linkage-specific α2,3 neuraminidase. Subsequent digestion by β4-specific galactosidase trimmed all Core 4 structures detected into a major trisaccharide, corresponding to the expected digestion product, GlcNAcβ1-3(GlcNAcβ1-6)GalNAcitol. It can thus be concluded from these data that all other minor components detected (Fig. 1) are incompletely extended and/or sialylated Core 4 structures.

MALDI-MS mapping and sequencing of RSL *N*-glycans

The MALDI-MS mapping and MS/MS sequencing of the RSL *O*-glycans described above clearly show that the major Cores 3 and 4 structures identified cannot account for the Man and Fuc detected in the overall glycosyl compositional analysis. Even after trimming away all the terminal α3-sialylation and β4-galactosylation, no additional component was detected apart from the expected digestion products. These data therefore suggest that the Man and Fuc are not carried on the *O*-glycans, but most likely on the *N*-glycans. In fact, several major glycans were released and detected by MALDI-MS analysis (Fig. 4) when the tryptic digested peptides from RSL were subjected to PNGase F treatment.

Curiously, the molecular ion signals at *m/z* below 2,000 could not be assigned to a composition consistent with *N*-glycan but resemble more the identified *O*-glycans instead. Further MS/MS sequencing confirmed that these were indeed the same *O*-glycan structures as those directly released by reductive elimination. Thus it is likely that a significant portion of heavily *O*-glycosylated peptides was too hydrophilic to be retained on reverse phase C18 solid phase and thus collected together with the released *N*-glycans in the aqueous wash fraction. The *O*-glycans would then be non-reductively released directly during the NaOH-based permethylation. By a similar process, it is possible that additional *O*-glycans might also be released directly during permethylation from the RSL sample that has already been subjected to direct reductive elimination, but which did not completely release all attached *O*-glycans. The non-reduced *O*-glycans thus produced would have 16 mass units lower than the reduced counterparts, which were visibly present in the spectra of *O*-glycans (Fig. 1) and *N*-glycans (Fig. 4).

Other than the *O*-glycan signals, the two major $[M+Na]^+$ molecular ions at *m/z* 2,563 and 2,389 can be assigned to NeuAc-sialylated, non-bisected, hybrid type *N*-glycans, with and without core fucosylation, respectively, based on

Fig. 2 MALDI TOF/TOF MSMS sequencing of permethylated Cores 1 and 2 *O*-glycan standards. Monosialylated Core 1 (**a**) and disialylated Core 1 (**b**) *O*-glycan standards were prepared from bovine fetuin whereas the disialylated Core 2 (**c**) *O*-glycan standards were obtained from HOC350, as described in the "Materials and methods." The high energy CID MS/MS cleavage patterns established are schematically illustrated on the respective structures. Nomenclature adopted for the various ions is based on that proposed by Domon and Costello [33], Spina *et al*. [20] and Yu *et al*. [22], and the assigned major peaks are *annotated* accordingly. Importantly for linkage assignment, the D ion is formed through a glycosidic cleavage in concert with elimination of the 3-substituent, which can be viewed as an internal cleavage ion arising through a combination of B/Y or C/Z type of cleavages [50]. The G ion is derived from concerted elimination of the attached C3 and C4 substituent [20], whereas the satellite H ion was assigned to similar elimination of the C4 and C6 substituents [22]. For a 4-linked HexNAc, the respective G and H ions will therefore differ by 14 mass units and can be identified as a characteristic pair of signals. Unusual ions or those not systematically named are further illustrated with additional schematic drawings. The sodiated B_1 ion for NeuAc at *m/z* 398 is often accompanied by the more abundant oxonium ions at *m/z* 376 and 344 (minus a MeOH moiety). The C_2 ion at *m/z* 620 is invariably paired with the minus 2 units C″ ion at *m/z* 618 for the NeuAc-Gal fragment. Loss of terminal NeuAc gave a characteristic doublet of two mass units apart, corresponding to $^{1,5}X$ and $^{O,2}X$ ion, usually accompanied by another signal at 16 mass units lower which was consistently observed, but not yet rationally assigned, *e.g*. *m/z* 590 with 604/606 in (**a**), *m/z* 951 with 965/967 in (**b**) and *m/z* 1,400 with 1,414/1,416 in (**c**). The signal at *m/z* 472 in (**c**) could be assigned to $^{1,3}A_2$ or $^{2,4}A_2$ ion of a NeuAc-3Gal- terminal epitope but is more likely to be derived from further loss of NeuAc from the sialylated Hex-HexNAc antenna to give a sodiated B/Y ion of (HO)Hex-HexNAc, since it was not observed in (**b**). Likewise, the signal at *m/z* 506 could be assigned to double cleavage ion of (OH)Hex-(OH)HexNAcitol

systematically identifying the characteristic ion series afforded by high energy CID MS/MS analyses (Fig. 5). For the non-fucosylated structure, the $^{1,5}X$ ion series at *m/z* 2100, 1838, 1593 and 1389 defines a NeuAc-Hex-HexNAc-Hex- terminal sequence, whereas the additional $^{1,5}X$ ions at *m/z* 2,199 and 1,791 correspond to loss of one and three Hex residues, respectively, from a non-reducing terminus, which is consistent with a branched Hex-(Hex)Hex- sequence as would be expected for the 6-arm of a hybrid type *N*-glycan (Fig. 5a). The next $^{1,5}X$ ion in series is found at *m/z* 573, arising from cleavage at the 3,6-branched β-Man. Similar $^{1,5}X$ ion series was afforded by the fucosylated structure, with the *m/z* values of each shifted to one Fuc (174 mass unit) higher (Fig. 5b), therefore confirming the overall identical sequence and placing the extra Fuc substituent at the chitobiose core. Indeed, a critical Y_1 ion at *m/z* 474 firmly establishes a core fucosylation at the reducing end HexNAc.

For more definitive assignment of the antennary distribution, the trio of $^{O,4}A$, $^{3,5}A$ and D ions at *m/z* 709, 737 and 839, respectively, collectively define the 6-arm as retaining the branched trimannosyl residues and therefore the extension on the 3-arm as NeuAc-Hex-HexNAc, for both structures. This is corroborated by the G ion resulting from

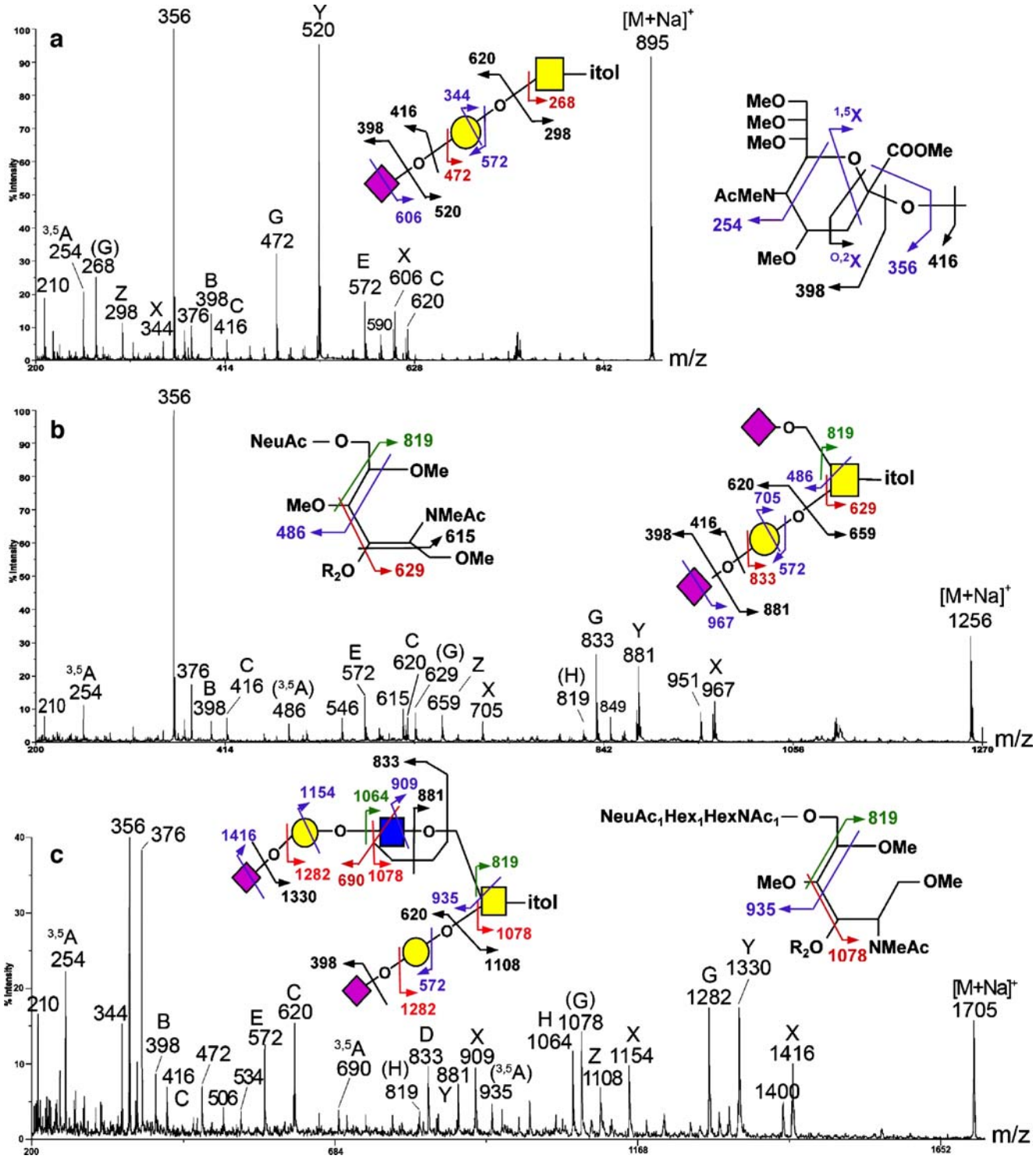

concerted elimination of the C3 and C4 substituents from the β-Man at *m/z* 1,313 and 1,487, for the respective two structures. As in the case of the *O*-glycans, the Gal-4GlcNAc linkage can be established from the respective G, H, ^{3,5}A, and D ions (see drawings on Fig. 5), whereas the NeuAc-3Gal linkage can be inferred from the presence of G ions at *m/z* 1966 and 2140. However, the additional presence of a D ion at *m/z* 588 is indicative of the co-existence of NeuAc-6Gal linkage, which is supported by non-complete removal of the sialic acids by α2,3-neuraminidase, unlike the situation with the *O*-glycans. The resistant product still afforded the D ion at *m/z* 588, but no longer gave the G ion at *m/z* 1966 and 2140. Accordingly, both 3-linked Gal and 6-linked Gal were detected by GC-MS linkage analysis of

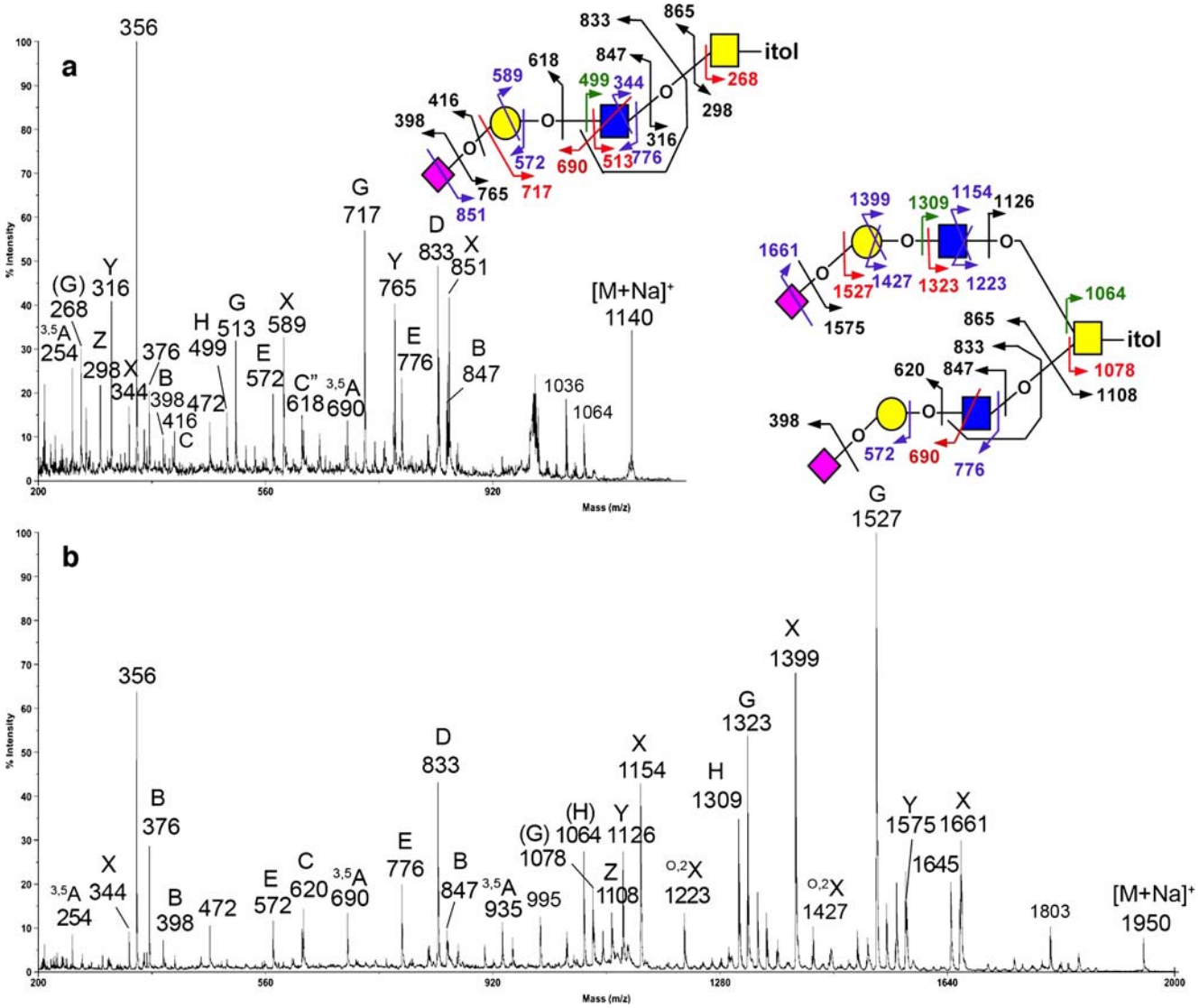

Fig. 3 MALDI TOF/TOF MSMS sequencing of permethylated RSL *O*-glycans. The parent ions selected for MS/MS correspond to $[M+Na]^+$ of $NeuAc_1Hex_1HexNAc_1$-HexNAc-itol at *m/z* 1,140 (**a**) and $NeuAc_2Hex_2$-$HexNAc_2$-HexNAc-itol at *m/z* 1,950 (**b**). Major signal assignments are schematically illustrated on the respective structures and critical ions are described in the text. For simplicity, not all assignable peaks were annotated. The H ion equivalent (*m/z* 1,064) for cleavages at the GalNAcitol appears to be more readily formed with the Cores 3 and 4 structures, compared to Cores 1 and 2 (*m/z* 819 in Fig. 2). The two signals of unknown origins at *m/z* 1,036 in (**a**) and 1,803 in (**b**) were not reproducibly formed and would likely to represent a loss of fragment less than a glycosyl residue

this sample prior to enzymatic desialylation (Table 1), along with terminal Man, 2-linked Man, and 3,6-linked Man, and the absence of 3,4,6-linked Man, which are fully supportive of the non-bisected hybrid type *N*-glycans.

In summary, our structural data unambiguously identify a sialylated type II chain, NeuAc-Galβ1-4GlcNAc as the major terminal epitope presented by RSL, as carried on both *O*- and *N*-glycans (Fig. 6). On the *O*-glycans, the predominant structure is biantennary-like on a Core 4 type structure, carrying two NeuAcα2-3Galβ1-4GlcNAc antennae, accompanied by lesser amount of monoantennary linear Core 3 type structure. On the *N*-glycans, both α3 and α6-sialylation are present and a single sialylated type II chain is carried on non-bisected, hybrid type structures, with and without core fucosylation. Interestingly, neither high mannose type nor complex type structures were detected although hybrid type structures with two sialylated type II chains on the 3-arm appeared to be also present at much lower abundance.

Interaction of RSL with applied lectins

Consistent with the major structures identified for the RSL, a poorly sialylated RSL after removal of 78% of the sialic acid (asialo-RSL) showed substantially increased binding

Table 1 GC-MS linkage analysis of the partially methylated alditol acetates from the *N*-glycans and *O*-glycans of RSL

Elution time (min)	Characteristic fragment ions	Assignment[a]	*N*-linked glycans[b]	*O*-linked glycans
14.02	118, 131, 162, 175	t-Fuc	+	−
15.51	118, 129, 145, 161, 162, 205	t-Man	+	−
16.63	129, 130, 161, 190	2-Man	+	−
16.97	118, 129, 161, 234	3-Gal	+	+
17.47	118, 129, 162, 189, 233	6-Gal	+	−
17.92	130, 246, 290	3-GalNAc-itol	−	+
18.42	118,129,189, 234	3,6-Man	+	−
19.72	130, 246, 318	3,6-GalNAc-itol	−	+
20.15	117, 159, 233	4-GlcNAc	+	+
21.45	117, 159, 261	4,6-GlcNAc	+	−
22.12	117, 129, 159, 189, 275, 346	3,6-GalNAc	+	−

[a] The respective partially methylated alditol acetates were identified by elution time and their characteristic fragment ions afforded by standard EI-MS analysis, in comparison to authentic standards.
[b] The permethylated *N*-glycan sample used for GC-MS linkage analysis additionally contained the non-reduced *O*-glycans, as shown by MALDI-MS analysis (Fig. 4).

activities toward many Galβ1→4GlcNAc (type II) active lectins, indicating that Galβ1→4GlcNAcβ1→3 (type II) is the reactive glycotope (Table 2) [35]. For the presence of Man in the context of hybrid type *N*-glycans, the purified RSL reacted best with *Morniga M*, moderately with PSA, and weakly with lentil, among the three Man specific lectins tested. Interestingly, asialo-RSL reacted strongly with all three Man specific lectins (Table 2), therefore suggesting that sialylation of the single type II chain on the 3-arm may contribute to some shielding effects towards the reactivity of the mannoses on the 6-arm. Inhibition assay against the lectin-carbohydrate interaction further demonstrated that asialo-RSL, as the most potent inhibitor, was 2.5×10^3 and 1.0×10^3 times more active than Man and a trimannosyl core of *N*-glycan (Tri-II), respectively, on a nanogram basis, whereas RSL was only about one fifth as active as its asialo-product (data not shown).

Discussion

The RSL sample used in this study was isolated from the small sublingual gland embedded in the submaxillary tissue and purified by the methods described by Moschera and Pigman [16]. It was found to be homogeneous by analytical ultracentrifugation and have a high molecular mass of 2.2×10^6. The carbohydrate content was determined to be as high as 81% (*w*/*w*), to which fucose and mannose contributed

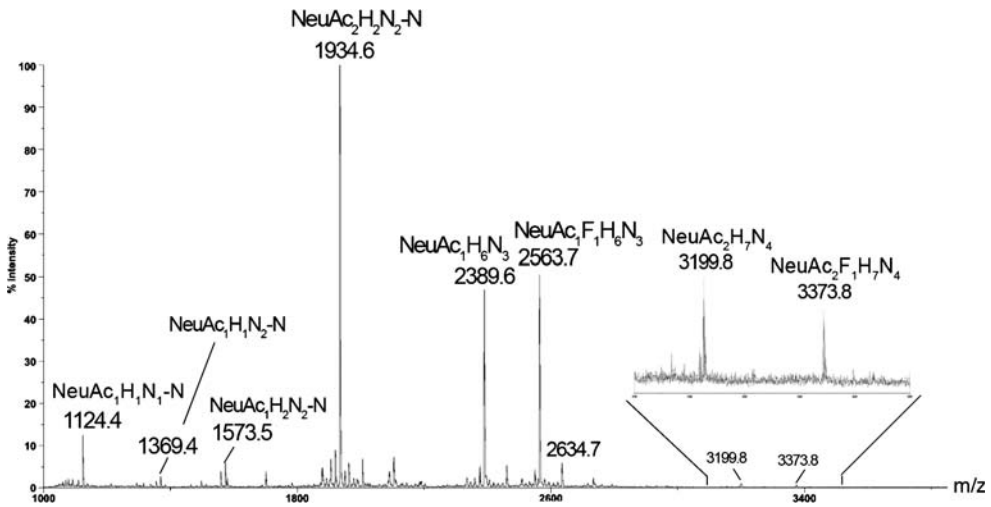

Fig. 4 MALDI-MS profile of permethylated RSL *N*-glycans. The molecular compositions of the major $[M+Na]^+$ molecular ion signals detected are assigned as labeled, and confirmed by subsequent MS/MS analysis. The signals at *m*/*z* lower than 2,000 correspond to the *O*-glycans identical to those released by direct reductive elimination (Fig. 1). Two additional weak signals at *m*/*z* 3,199 and 3,373 correspond to a NeuAc-Hex-HexNAc increment from the respective two major *N*-glycans and are likely to represent the same hybrid type structures with an additional antenna on the 3-arm although their exact identities were not further investigated due to low abundance

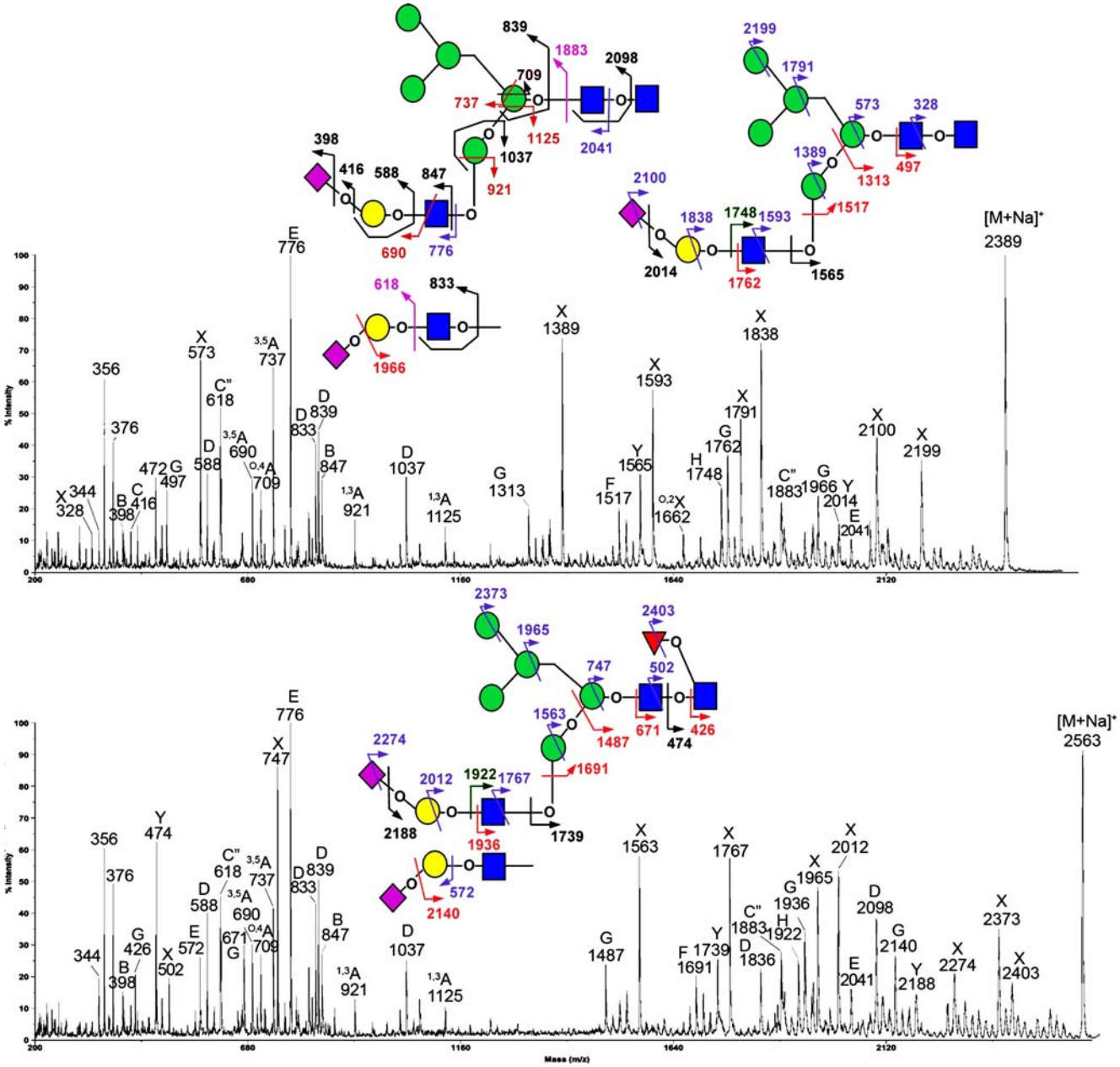

Fig. 5 MALDI TOF/TOF MSMS sequencing of permethylated RSL *N*-glycans. The parent ions selected for MS/MS correspond to $[M+Na]^+$ of $NeuAc_1Hex_6HexNAc_3$ at *m/z* 2389 (**a**) and $NeuAc_1Hex_6HexNAc_3Fuc_1$ at *m/z* 2,563 (**b**). Major signal assignments are schematically illustrated on the respective structures and critical ions are described in the text. For simplicity, not all assignable peaks were annotated

about 1.2 and 2.8% (*w*/*w*), respectively, with the remaining glycosyl composition made up of sialic acid, GlcNAc, GalNAc and Gal, in the molar ratio of 1.7:1.7:1.2:1.8 per mol of alkali-borohydride-labile hydroxyamino acid [16]. With the current knowledge that the minor amount of Fuc and Man can all be attributed to *N*-glycans, the derived molar ratio is remarkably close to that expected for the single major *O*-glycan identified, namely, NeuAcα2-3Galβ1-4GlcNAcβ1-3(NeuAcα2-3Galβ1-4GlcNAcβ1-6)GalNAc. Furthermore, considering that each *O*- and *N*-glycan chain on RSL can be represented by a single GalNAc and 5 Man residues, respectively, their molar ratio can be estimated to be 17.4, with about 1,342 *O*-glycan chains and 77 *N*-glycan chains per molecule of RSL, or about one glycan chain per 2–3 amino acids, based on the estimated average molecular masses of 2.2×10^6 and 115 for the RSL preparation and individual amino acid residue, respectively. This calculation would place RSL as one of

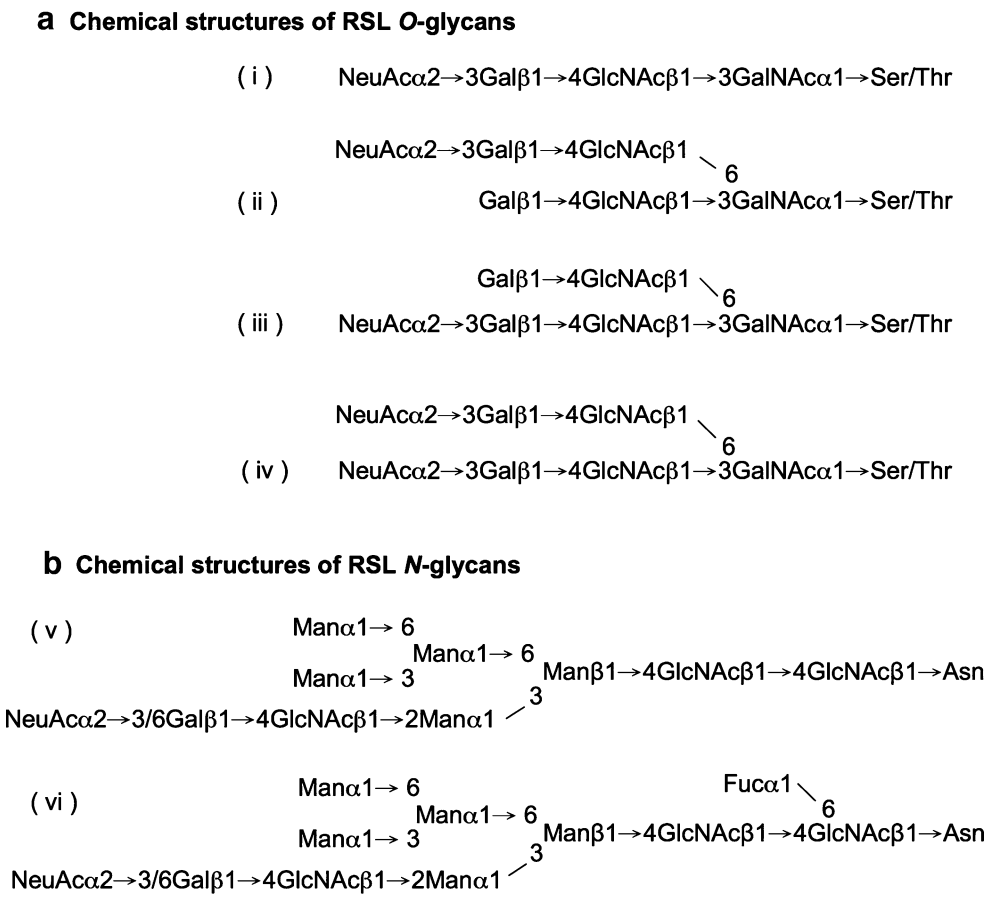

Fig. 6 Major glycan structures of rat sublingual glycoprotein established in this study. The major *O*-glycans (**a**) are based on Cores 3 (*i*) and 4 (*ii–iv*), dominated by a single most abundant disialylated Core 4 structure (*iv*). The major *N*-glycans (**b**) are non-bisected hybrid type structures, with (*vi*) and without (*v*) core fucosylation

the most heavily glycosylated glycoproteins that have been characterized.

Remarkably then, both the *N*- and *O*-glycosylation of RSL are dominated by a single preferred structure, with respect to core type and terminal sequence. Although Cores 3 and 4 are not that uncommon among the mucin *O*-glycans, its exclusive occurrence without any appreciable amount of the more ubiquitous Cores 1 and 2, as in the case

Table 2 Comparative binding activities of native and asialo-RSL with various lectins by ELLSA

Lectin[a]	Determinants[b] (Carbohydrate specificities)	Amount of lectin (ng)	1.5 (A_{405}) unit (ng)		Maximum A_{405} absorbance[c]		Binding intensity[c]	
			Native RSL	Asialo-RSL	Native RSL	Asialo-RSL	Native RSL	Asialo-RSL
Galβ1→4GlcNAc (type II) specific lectins								
RCA_1	II>I>B>T>>Tn	5	−	1.5	0.07	4.4	−	5+
ECL	I/II>B>Tn	10	−	15.0	0.02	4.2	−	5+
ECorL	I/II>B>Tn	50	−	25.0	0.02	4.2	−	5+
Mannose specific lectins								
Morniga M	Man	20	70.0	3.0	2.6	4.0	5+	5+
PSA	Man	200	900.0	30.0	1.1	3.1	2+	5+
Lentil	Man	50	−	55.0	0.2	2.9	±	5+

[a] Abbreviations for lectins used and binding data were adapted from Wu *et al*. [24, 38].

[b] Carbohydrate specificity of lectins as expressed by lectin determinants—type *I/II*, Galβ1→3/4GlcNAc; B, Galα1→3Gal; *T*, Galβ1→3GalNAc; *Tn*, GalNAcα1→Ser/Thr [38, 53]. The carbohydrate specificity of the Man specific lectins was defined against the trimannosyl core structure in *N*-linked glycoprotein [24].

[c] Maximum A_{405} is the maximum absorbance intensity recorded at the given quantity of the glycoprotein and lectin at wavelength 405 nm. Results were interpreted according to the measured A_{405} after 2 h (for Morniga M) or after 4 h (for all other lectins used) of incubation as follows: 5+ (OD≥2.5), 4+ (2.5>OD≥2.0), 3+ (2.0>OD≥1.5), 2+ (1.5>OD≥1.0), 1+ (1.0>OD≥0.5), ± (0.5>OD≥0.2), and − (OD<0.2).

of the RSL *O*-glycans, is rare. It remains to be tested if the observed glycomic profile can be correlated with the expressed activities of Core 3 synthase relative to that of Core 1 synthases in rat sublingual gland. In human, the Cores 3 and 4 are known to exhibit a rather restricted, organ-specific expression pattern [10], particularly along the intestinal tract [36]. Notably, almost all of the normal human colonic mucin *O*-glycans are based on Core 3 [37–39], which has been shown to be down-regulated and replaced by Cores 1 and 2 structures in colonic carcinomas [40]. However, none of the human and other mammalian salivary mucins characterized to date [1–4, 6, 41–45] show a similar strict preference for Cores 3 and 4 structures, particularly for a single predominant Core 4 structure, as carried on the RSL.

Likewise, it is unusual to find only the non-bisected hybrid type *N*-glycans without the presence of high mannose or complex types. A recent work on the *N*-glycans from endogenous MUC1 derived from human milk and a recombinant epitope-tagged variant overexpressed in Caco2 colon carcinoma cells demonstrated that *N*-glycosylation on MUC1 from these two sources comprise a full range of high mannose, hybrid and complex type glycans [46]. In the case of mouse submandibular mucin *N*-glycans, the only reported structural studies of *N*-glycans from salivary mucins, the hybrid type structures were accompanied by high mannose types and the absence of α-mannosidase II activity has been suggested to account for the lack of complex type structures [15]. It appears that processing of high mannose structures is more complete in RSL but fell equally short of removing the last 2 mannoses, after GlcNAc transferase I initiated the antennae on the 3-arm. Thus, deficiency in completely processing the hybrid type *N*-glycans on salivary mucins into a full range of complex type structures may be more reflective of their biosynthetic origins. Additional heterogeneity on RSL *N*-glycans is, however, conferred by core fucosylation and α2–6 sialylation which are both absent from the mouse submandibular mucin *N*-glycans. Interestingly, sialylation on the major RSL *O*-glycans is found to be restricted to α2–3 linkage.

Regardless of the sialylation status, both the RSL *N*- and *O*-glycan cores are extended by type II chain, which is the single defining epitope revealed by probing against a panel of lectins. From previous results of enzyme-linked lectinosorbent (ELLSA) and inhibition assays [35], it was concluded that type II, or Galβ1→4GlcNAcβ1→, from both *O*- and *N*-glycans are the dominant glycotopes in asialo RSL, once the shielding effect of sialic acid on the subterminal sugar residue at the nonreducing ends is removed [35]. It can thus be used as an important reagent for detecting type II reactive lectins. In addition, asialo-RSL reacted strongly with Morniga M, and also bound the other two Man specific lectins well (Table 2), consistent with the presence of mannoses on the *N*-glycans albeit not as high mannose structures.

In conclusion, our current work provided the missing structural data that was implicated by previously reported glycosyl composition [16] and lectin binding studies [35]. The advanced mass spectrometry-based glycomic approach is powerful in that it not only gives an overall picture of the glycosylation complexity, but also furnishes detailed sequence, branching, and linkage information, without extensive fractionation and purification. In continuation from our own earlier work on the *N*-glycans [22], we have shown that the high energy CID fragmentation characteristics, in so far as the major ion series afforded, are equally applicable to the *O*-glycans. However, it would appear that ions derived from successive glycosidic cleavages such as that combining a B ion-cleavage at HexNAc with facile loss of terminal sialic acid are more readily formed. Nevertheless, in general, the fragmentation pattern still distinguishes itself from that afforded by low energy CID on Q/TOF in being mostly restricted to single glycosidic cleavages, complemented by cross ring cleavages and concerted elimination of two adjacent substituents around the pyranose ring. Additionally, all Cores 1–4 type structures readily afford the Z_1 ion due to the C3-linkage but not one with further loss of the 6-arm substituents, namely a $Z_{1\alpha}/Y_{1\beta}$ ion commonly given by Cores 2 and 4, or a $Y_{1\alpha}/Y_{1\beta}$ ion by Core 4, on a Q/TOF is not normally observed.

The highly abundant Core 4 structure given by the RSL *O*-glycans implies that the competing sialylation at the C6 of GalNAc is less favored in the presence of high Core 4 β6-GlcNAc transferase activity [40]. An early work focusing on an isolated fraction of the released *O*-glycans (11% of total) has led to identification of 5 structurally related Core 3 structures, deduced to be of the sequence (±NeuAcα2→4)GlcNAcβ1→3[(NeuAcα2→6)Galβ1→4GlcNAcβ1→3]$_{2-4}$(NeuAcα2→6)GalNAcitol, whereas the structures of the major components were not reported in the same study [47]. We have not been able to detect these highly unusual sialylated Core 3 structures in our current studies. Neither could these be identified in the corresponding *O*-glycan samples derived from asialo-RSL, whereby desialylation would have facilitated their detection by MS. In the absence of more definitive structural data, the representative major *O*-glycan structures of RSL should be revised accordingly from those represented in the current literature [7, 41], in the light of present work. We have shown that the 3,6-branched GalNAc at the reducing end is mainly derived from a Core 4 structure and not from a sialylated Core 3. Furthermore, a majority, if not all, of the sialylation on the *O*-glycans are represented by NeuAcα2-3Gal-. The previously proposed NeuAcα2→4GlcNAc- and →3(NeuAcα2→6)Gal-linkages [47] remain un-

substantiated and are not supported by our current knowledge of the existing mammalian sialyltransferases [48, 49].

Acknowledgement This study was supported by grants from the Chang-Gung Medical Research Project (CMRPD no. 33022) and the Taiwan National Science Council (NSC 94-2320-B-182-044, NSC 94-2320-B-182-053) to AMW; and a Taiwan NSC grant 95-3112-B-001-014 to the National Core Facilities for Proteomics, located at the Institute of Biological Chemistry, Academia Sinica.

References

1. Levine, M.J., Reddy, M.S., Tabak, L.A., Loomis, R.E., Bergey, E.J., Jones, P.C., Cohen, R.E., Stinson, M.W., Al-Hashimi, I.: Structural aspects of salivary glycoproteins. J. Dent. Res. **66**, 436–441 (1987)
2. Klein, A., Carnoy, C., Wieruszeski, J.M., Strecker, G., Strang, A.M., van Halbeek, H., Roussel, P., Lamblin, G.: The broad diversity of neutral and sialylated oligosaccharides derived from human salivary mucins. Biochemistry. **31**, 6152–6165 (1992)
3. Slomiany, B.L., Murty, V.L., Slomiany, A.: Structural features of carbohydrate chains in human salivary mucins. Int. J. Biochem. **25**, 259–265 (1993)
4. Ohmori, T., Toyoda, H., Toida, T., Imanari, T., Sato, H.: Comparison of oligosaccharides derived from salivary mucin of Japanese secretor and non-secretor individuals of blood group type-A. Glycoconj. J. **18**, 635–640 (2001)
5. Thomsson, K.A., Prakobphol, A., Leffler, H., Reddy, M.S., Levine, M.J., Fisher, S.J., Hansson, G.C.: The salivary mucin MG1 (MUC5B) carries a repertoire of unique oligosaccharides that is large and diverse. Glycobiology. **12**, 1–14 (2002)
6. Thomsson, K.A., Schulz, B.L., Packer, N.H., Karlsson, N.G.: MUC5B glycosylation in human saliva reflects blood group and secretor status. Glycobiology. **15**, 791–804 (2005)
7. Herp, A., Wu, A.M., Moschera, J.: Current concepts of the structure and nature of mammalian salivary mucous glycoproteins. Mol. Cell. Biochem. **23**, 27–44 (1979)
8. Wu, A.M., Shen, F., Herp, A., Wu, J.H.: Interaction of hamster submaxillary sialyl-Tn and Tn glycoproteins with Gal, GalNAc and GlcNAc specific lectins. Mol. Immunol. **31**, 485–490 (1994)
9. Van den Steen, P., Rudd, P.M., Dwek, R.A., Opdenakker, G.: Concepts and principles of *O*-linked glycosylation. Crit. Rev. Biochem. Mol. Biol. **33**, 151–208 (1998)
10. Hanisch, F.G.: *O*-glycosylation of the mucin type. Biol. Chem. **382**, 143–149 (2001)
11. Strous, G.J., Dekker, J.: Mucin-type glycoproteins. Crit. Rev. Biochem. Mol. Biol. **27**, 57–92 (1992)
12. Perez-Vilar, J., Hill, R.L.: The structure and assembly of secreted mucins. J. Biol. Chem. **274**, 31751–31754 (1999)
13. Denny, P.A., Denny, P.C.: A mouse submandibular sialomucin containing both *N*- and *O*-glycosylic linkages. Carbohydr. Res. **110**, 305–314 (1982)
14. Amerongen, A.V., Oderkerk, C.H., Roukema, P.A., Wolf, J.H., Lisman, J.J., Overdijk, B.: Murine submandibular mucin (MSM): a mucin carrying *N*- and *O*-glycosylically bound carbohydrate-chains. Carbohydr. Res. **115**, C1–5 (1983)
15. Denny, P.C., Denny, P.A., Hong-Le, N.H.: Characterization of asparagine-linked oligosaccharides on a mouse submandibular mucin. Glycobiology. **5**, 589–597 (1995)
16. Moschera, J., Pigman, W.: The isolation and characterization of rat sublingual mucus-glycoprotein. Carbohydr. Res. **40**, 53–67 (1975)
17. Wada, Y., Azadi, P., Costello, C.E., Dell, A., Dwek, R.A., Geyer, H., Geyer, R., Kakehi, K., Karlsson, N.G., Kato, K., Kawasaki, N., Khoo, K.H., Kim, S., Kondo, A., Lattova, E., Mechref, Y., Miyoshi, E., Nakamura, K., Narimatsu, H., Novotny, M.V., Packer, N.H., Perreault, H., Peter-Katalinic, J., Pohlentz, G., Reinhold, V.N., Rudd, P.M., Suzuki, A., Taniguchi, N.: Comparison of the methods for profiling glycoprotein glycans—HUPO human disease glycomics/proteome initiative multi-institutional study. Glycobiology. **17**, 411–422 (2007)
18. Jang-Lee, J., North, S.J., Sutton-Smith, M., Goldberg, D., Panico, M., Morris, H., Haslam, S., Dell, A.: Glycomic profiling of cells and tissues by mass spectrometry: fingerprinting and sequencing methodologies. Methods Enzymol. **415**, 59–86 (2006)
19. Morelle, W., Slomianny, M.C., Diemer, H., Schaeffer, C., van Dorsselaer, A., Michalski, J.C.: Fragmentation characteristics of permethylated oligosaccharides using a matrix-assisted laser desorption/ionization two-stage time-of-flight (TOF/TOF) tandem mass spectrometer. Rapid Commun. Mass Spectrom. **18**, 2637–2649 (2004)
20. Spina, E., Sturiale, L., Romeo, D., Impallomeni, G., Garozzo, D., Waidelich, D., Glueckmann, M.: New fragmentation mechanisms in matrix-assisted laser desorption/ionization time-of-flight/time-of-flight tandem mass spectrometry of carbohydrates. Rapid Commun. Mass Spectrom. **18**, 392–398 (2004)
21. Stephens, E., Maslen, S.L., Green, L.G., Williams, D.H.: Fragmentation characteristics of neutral *N*-linked glycans using a MALDI-TOF/TOF tandem mass spectrometer. Anal. Chem. **76**, 2343–2354 (2004)
22. Yu, S.Y., Wu, S.W., Khoo, K.H.: Distinctive characteristics of MALDI-Q/TOF and TOF/TOF tandem mass spectrometry for sequencing of permethylated complex type *N*-glycans. Glycoconj. J. **23**, 355–369 (2006)
23. Tettamanti, G., Pigman, W.: Purification and characterization of bovine and ovine submaxillary mucins. Arch. Biochem. Biophys. **124**, 41–50 (1968)
24. Wu, A.M., Wu, J.H., Singh, T., Chu, K.C., Peumans, W.J., Rouge, P., Van Damme, E.J.: A novel lectin (Morniga M) from mulberry (*Morus nigra*) bark recognizes oligomannosyl residues in *N*-glycans. J. Biomed. Sci. **11**, 874–885 (2004)
25. Duk, M., Lisowska, E., Wu, J.H., Wu, A.M.: The biotin/avidin-mediated microtiter plate lectin assay with the use of chemically modified glycoprotein ligand. Anal. Biochem. **221**, 266–272 (1994)
26. Nilsson, B., Norden, N.E., Svensson, S.: Structural studies on the carbohydrate portion of fetuin. J. Biol. Chem. **254**, 4545–4553 (1979)
27. Spiro, R.G., Bhoyroo, V.D.: Structure of the *O*-glycosidically linked carbohydrate units of fetuin. J. Biol. Chem. **249**, 5704–5717 (1974)
28. Wu, A.M., Wu, J.H., Watkins, W.M., Chen, C.P., Tsai, M.C.: Binding properties of a blood group Le(a+) active sialoglycoprotein, purified from human ovarian cyst, with applied lectins. Biochim. Biophys. Acta. **1316**, 139–144 (1996)
29. Lisowska E.D.M., Wu AM. (1996) Preparation of biotinylated lectins and application in microtiter plate assays and Western blotting. Vol. 7
30. Dell, A., Reason, A.J., Khoo, K.H., Panico, M., McDowell, R.A., Morris, H.R.: Mass spectrometry of carbohydrate-containing biopolymers. Methods Enzymol. **230**, 108–132 (1994)
31. Wu, A.M., Pigman, W.: Preparation and characterization of armadillo submandibular glycoproteins. Biochem. J. **161**, 37–47 (1977)
32. Ciucanu, I., Kerek, F.: A simple and rapid method for the permethylation of carbohydrates. Carbohydr. Res. **131**, 209–217 (1984)

33. Domon, B., Costello, C.E.: Structure elucidation of glycosphingolipids and gangliosides using high-performance tandem mass spectrometry. Biochemistry. **27**, 1534–1543 (1988)
34. Mechref, Y., Kang, P., Novotny, M.V.: Differentiating structural isomers of sialylated glycans by matrix-assisted laser desorption/ionization time-of-flight/time-of-flight tandem mass spectrometry. Rapid Commun. Mass Spectrom. **20**, 1381–1389 (2006)
35. Wu, A.M., Herp, A., Song, S.C., Wu, J.H., Chang, K.S.: Interaction of native and asialo rat sublingual glycoproteins with lectins. Life Sci. **57**, 1841–1852 (1995)
36. Robbe, C., Capon, C., Coddeville, B., Michalski, J.C.: Structural diversity and specific distribution of *O*-glycans in normal human mucins along the intestinal tract. Biochem. J. **384**, 307–316 (2004)
37. Podolsky, D.K.: Oligosaccharide structures of human colonic mucin. J. Biol. Chem. **260**, 8262–8271 (1985)
38. Podolsky, D.K.: Oligosaccharide structures of isolated human colonic mucin species. J. Biol. Chem. **260**, 15510–15515 (1985)
39. Capon, C., Maes, E., Michalski, J.C., Leffler, H., Kim, Y.S.: Sd (a)-antigen-like structures carried on core 3 are prominent features of glycans from the mucin of normal human descending colon. Biochem. J. **358**, 657–664 (2001)
40. Brockhausen, I.: Pathways of *O*-glycan biosynthesis in cancer cells. Biochim. Biophys. Acta. **1473**, 67–95 (1999)
41. Herp, A., Borelli, C., Wu, A.M.: Biochemistry and lectin binding properties of mammalian salivary mucous glycoproteins. Adv. Exp. Med. Biol. **228**, 395–435 (1988)
42. Savage, A.V., Donoghue, C.M., D'Arcy, S.M., Koeleman, C.A., van den Eijnden, D.H.: Structure determination of five sialylated trisaccharides with core types 1, 3 or 5 isolated from bovine submaxillary mucin. Eur. J. Biochem. **192**, 427–432 (1990)
43. Chai, W.G., Hounsell, E.F., Cashmore, G.C., Rosankiewicz, J.R., Bauer, C.J., Feeney, J., Feizi, T., Lawson, A.M.: Neutral oligosaccharides of bovine submaxillary mucin. A combined mass spectrometry and 1H-NMR study. Eur. J. Biochem. **203**, 257–268 (1992)
44. Slomiany, B.L., Murty, V.L.N., Piotrowski, J., Slomiany, A.: Salivary mucins in oral mucosal defense. Gen. Pharmacol. **27**, 761–771 (1996)
45. Zalewska, A., Zwierz, K., Zolkowski, K., Gindzienski, A.: Structure and biosynthesis of human salivary mucins. Acta Biochim. Pol. **47**, 1067–1079 (2000)
46. Parry, S., Hanisch, F.G., Leir, S.H., Sutton-Smith, M., Morris, H.R., Dell, A., Harris, A.: *N*-Glycosylation of the MUC1 mucin in epithelial cells and secretions. Glycobiology. **16**, 623–634 (2006)
47. Slomiany, A., Slomiany, B.L.: Structures of the acidic oligosaccharides isolated from rat sublingual glycoprotein. J. Biol. Chem. **253**, 7301–7306 (1978)
48. Dall'Olio, F., Chiricolo, M.: Sialyltransferases in cancer. Glycoconj. J. **18**, 841–850 (2001)
49. Harduin-Lepers, A., Vallejo-Ruiz, V., Krzewinski-Recchi, M.-A., Samyn-Petit, B., Julien, S., Delannoy, P.: The human sialyltransferase family. Biochimie. **83**, 727–737 (2001)
50. Harvey, D.J., Bateman, R.H., Green, M.R.: High-energy collision-induced fragmentation of complex oligosaccharides ionized by matrix-assisted laser desorption/ionization mass spectrometry. J. Mass Spectrom. **32**, 167–187 (1997)